Einstein-Podolsky-Rosen steering and monogamy relations in controllable dynamical Casimir arrays

Mengxin Zhang, Yumei Long, Shiqing Zhao, and Xue Zhang [*]
Center for Quantum Sciences and School of Physics, Northeast Normal University, Changchun, 130024, China and Center for Advanced Optoelectronic Functional Materials Research, and Key Laboratory for UV-Emitting Materials and Technology of Ministry of Education, Northeast Normal University, Changchun, 130024, China

(Received 24 June 2021; accepted 12 April 2022; published 27 April 2022)

We achieve the controllable multipartite Einstein-Podolsky-Rosen (EPR) steering and its monogamy relations by means of the dynamical Casimir effect in the frame of superconducting quantum network. We employ the external driving flux of the superconducting quantum interference device as a switch. It is interesting that the system exhibits different types of the EPR steering and monogamy relations by tuning parameters. In the system, the one-way or two-way EPR steerings for different parties have been realized, and the direction of the one-way EPR steering is reversed by tuning coupling parameters. Remarkably, we can also obtain the EPR steering orderly sudden death for different modes. In addition, the system not only shows the type-I and type-II monogamy relations, but also converts steering parties to get monogamy relations' swapping and cycling. Finally, we discuss the influence of temperature. In the system, the higher the temperature is, the earlier sudden death for the EPR steering is. These results are important for quantum information and lay a foundation for us to better understand the important role of the multipartite EPR steering in secure quantum communication.

DOI: 10.1103/PhysRevA.105.042435

I. INTRODUCTION

The dynamical Casimir effect (DCE) [1,2] is the phenomenon that pairs of photons are generated due to the nonadiabatic change of boundary condition [3,4] or refractive index [5,6]. The DCE was observed experimentally for the first time in superconducting quantum circuit modulated by superconducting quantum interference device (SQUID) [7]. Since the photon pairs generated by the DCE are nonclassical [8], the DCE is used as a coherent light source to study the quantum correlations such as entanglement [9–13] and Einstein-Podolsky-Rosen (EPR) steering [14–21].

More discussions about the DCE were reported in Ref. [22] in the superconducting quantum circuit. The superconducting quantum circuit has attracted much attention because of its excellent controllability and integration [23–25]. In addition to the experimental observation for the DCE, many physicists also considered the superconducting quantum circuit as a tool to study Unruh effects [22], Hawking radiation [22], state transition in off-resonant coupling [26], and quantum communication [11,27]. In this paper, based on the superconducting quantum circuit which generates the DCE, we design more complex dynamical Casimir arrays (DCA) shown in Fig. 1 to study the multipartite EPR steering and its monogamy relations [28–30].

It is necessary to discuss the EPR steering before introducing the multipartite EPR steering. The word "steering" was first proposed by Schrödinger [31] to represent the phenomenon "a distanced spooky action" exhibited in famous EPR paradox [32,33]. The EPR steering is an intermediate quantum correlation between quantum entanglement [9–13] and Bell nonlocality [34,35], where the local measurement on Alice can steer the state of Bob [16,17,36,37]. This correlation indicates connatural asymmetric feature, which mainly contributes to the subchannel discrimination [38], one-sided device-independent quantum cryptography [39–43], and quantum teleportation [44–46]. Multipartite EPR steering contains distinct parties that cannot be absolutely trusted. Recently, the multipartite EPR steering is regared as a critical source for secure quantum communication. However, only one party can share this source, that is, two diverse parties cannot steer the third one simultaneously. The property is called the monogamy of multipartite EPR steering. He *et al.* have introduced the monogamy relations by means of three

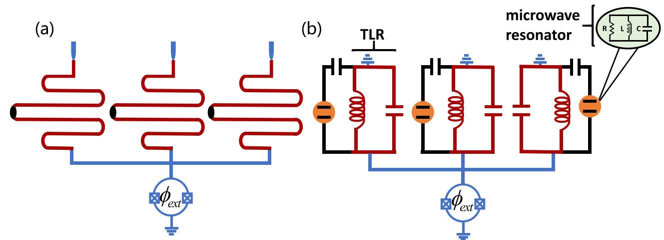

FIG. 1. (a) Diagram of the system, consisting of three subsystems that are composed of finite coplanar waveguides and resonant microwave resonators. Three coplanar waveguides are grounded through a SQUID. (b) Diagram of the circuit. TLRs are described by LC oscillation circuits and RLC resonators are represented by inductor, capacitor, and resistor.

[*]zhangx800@nenu.edu.cn

cascaded four-wave mixing (FWM) processes [28,29]. Instead, we choose superconducting quantum circuit to study monogamy relations of multipartite EPR steering.

In this paper, on the basis of the superconducting circuit framework (Fig. 1), with the help of perturbation theory and the EPR steering criterion [33,36], we study the multipartite EPR steering and discuss the corresponding monogamy relations [28,29]. The controllable external driving flux of the SQUID results in the controllable EPR steering and monogamy relations. In such a well-designed system, there are some interesting phenomena. We have achieved the one-way or two-way EPR steering generation and orderly sudden death, and the direction of the one-way EPR steering can be reversed by controllable parameter inversion. On the other hand, based on the multipartite EPR steering, the system exhibits type-I and type-II monogamy relations, and the monogamy relations' swapping and cycling can also be obtained with the adjustment of detunings or coupling parameters.

The structure of this paper is as follows. In Sec. II, we present the model and its Hamiltonian. We show the results and discussion in Sec. III, in which Sec. III A introduces the perturbative results, Sec. III B exhibits the multipartite EPR steering criterion, Sec. III C discusses the multipartite EPR steering in the DCA, Sec. III D discusses the monogamy relations of the multipartite EPR steering in the DCA, and Sec. III E shows the influence of temperature on the system. We summarize this paper in Sec. IV.

II. MODEL AND HAMILTONIAN

We study the system depicted in Fig. 1(a), consisting of three finite coplanar waveguide-microwave resonator subsystems. In the subsystem, the microwave resonator is a parallel resistor-inductor-capacitor (RLC) resonator, which is strongly coupled with the transmission line resonator (TLR), as shown in Fig. 1(b). The TLRs interact with each other through a superconducting quantum interference device (SQUID) [47]. Changing the external magnetic flux ϕ_{ext} of SQUID generates the time-dependent boundary conditions.

The Hamiltonian describing the above system is written as

$$\begin{aligned} H = &\hbar \sum_{k=1}^{3} (\Omega_k a_k^\dagger a_k + \omega_k b_k^\dagger b_k) \\ &+ \hbar \sum_{k=1}^{3} G_k (b_k^\dagger a_k + b_k a_k^\dagger) \\ &+ \hbar \sum_{\langle k.l\rangle} \beta_{k,l}(t)(a_k^\dagger + a_k)(a_l^\dagger + a_l). \end{aligned} \tag{1}$$

The subscript k represents different subsystems, $a_k^\dagger$ and a_k are the creation and annihilation operators of the TLR modes with characteristic frequency Ω_k, and $b_k^\dagger$ and b_k represent the creation and annihilation operators of the RLC resonator modes with characteristic frequency ω_k. In Eq. (1), the second line contains three different energy-exchange interactions, each TLR resonantly interacts with the corresponding RLC resonator with the strength G_k. The third line represents the interaction of the different TLR, and $\beta_{k,l}(t)$ is the coupling strength between kth TLR mode and lth TLR mode.

It should be noted that the driving frequency of SQUID Ω_d must be less than its plasma frequency Ω_p, therefore, the external flux $\phi_{ext}(t)$ of SQUID is written as [11]

$$\frac{\phi_{ext}}{2\varphi_0} = \bar{\phi} + \sum_{\langle k,l\rangle} \Delta_{k,l} \cos\left(\Omega_d^{k,l} t\right), \tag{2}$$

with $\bar{\phi}$ is a constant offset and $\Delta_{k,l}$ is little variation, $\varphi_0 = \phi_0/2\pi$, ϕ_0 is magnetic flux quantum. The time-dependent coupling parameter $\beta_{k,l}(t)$ is given by [11]

$$\beta_{k,l}(t) = \beta_0^{k,l} \cos\left(\Omega_d^{k,l} t\right), \tag{3}$$

where

$$\beta_0^{k,l} = \frac{\varphi_0^2}{4E_J} \frac{\sin\bar{\phi}}{\cos^2\bar{\phi}} \sqrt{\frac{\Omega_k \Omega_l}{C_k C_l}} \frac{I}{Z_k Z_l} \Delta_{k,l}, \tag{4}$$

and C_k and Z_k are corresponding capacitance and impedance of TLR$_k$. According to Eqs. (2) and (4), controllable ϕ_{ext} allows us to obtain tunable driving frequency and coupling strength $\beta_0^{k,l}$. Turning off the external flux of SQUID at reasonable time, the external driving and interaction of the TLRs will disappear.

III. RESULTS AND DISCUSSION

A. Perturbative results

When the system satisfies the condition $\beta_0^{k,l}/\Omega_k \ll 1$, we can ignore the fast-oscillating term and go to the interaction frame by means of rotating-wave approximation [11,48]. Therefore, in the interaction picture Eq. (1) is rewritten as [11]

$$\begin{aligned} H_{\text{eff}} = &\hbar \sum_{k=1}^{3} G_k (b_k^\dagger a_k + b_k a_k^\dagger) + \frac{\hbar}{2}\big(\beta_0^{1,2} a_1^\dagger a_2^\dagger e^{i(\Omega_1+\Omega_2)t} \\ &+ \beta_0^{2,3} a_2^\dagger a_3^\dagger e^{i(\Omega_2+\Omega_3)t} + \beta_0^{1,3} a_1^\dagger a_3 e^{i(\Omega_1-\Omega_3)t} + \text{H.c.}\big). \end{aligned} \tag{5}$$

We use the perturbative theory to derive the state $|\Phi(t)\rangle$ expanded up to the third order from state $|000\rangle_{\text{TLR}} \otimes |000\rangle_q$ under Eq. (5), where $|0\rangle$, $|1\rangle$, $|2\rangle$, and $|3\rangle$ are Fock-number states of TLRs and RLC resonators. $|\Phi(t)\rangle$ has projections into the state $|\varphi_n\rangle$, $|\varphi_n\rangle$ is specifically written as $|000\rangle_{\text{TLR}} \otimes |m\rangle_q$ $(m = 110, 011)$, $|n\rangle_{\text{TLR}} \otimes |001\rangle_q$, $|n\rangle_{\text{TLR}} \otimes |100\rangle_q$ $(n = 010, 021, 120)$, $|x\rangle_{\text{TLR}} \otimes |000\rangle_q$ $(x = 000, 110, 011, 022, 220, 330, 033, 132, 231, 121)$, and $|y\rangle_{\text{TLR}} \otimes |010\rangle_q$ $(y = 001, 100, 111, 012, 210)$.

$|\Phi(t)\rangle$ can be written as a linear superposition of the $|\varphi_n\rangle$. In terms of the average value formula, we present all average values expressed in the EPR criteria in the system. Some are shown here, and the rest of the values are shown in the Appendix:

$$\begin{aligned} &\langle b_1 b_3\rangle = \langle b_3 b_1\rangle = 0, \\ &\langle b_1 b_2\rangle = f^{(0,2,3)*}_{|000\rangle_{\text{TLR}}\otimes|000\rangle_q} f^{(3)}_{|000\rangle_{\text{TLR}}\otimes|110\rangle_q}, \\ &\langle b_2 b_1\rangle = f^{(0,2,3)*}_{|000\rangle_{\text{TLR}}\otimes|000\rangle_q} f^{(3)}_{|000\rangle_{\text{TLR}}\otimes|110\rangle_q}, \\ &\langle b_2 b_3\rangle = f^{(0,2,3)*}_{|000\rangle_{\text{TLR}}\otimes|000\rangle_q} f^{(3)}_{|000\rangle_{\text{TLR}}\otimes|011\rangle_q}, \end{aligned}$$

$$\langle b_3 b_2\rangle = f^{(0,2,3)*}_{|000\rangle_{\mathrm{TLR}}\otimes|000\rangle_q} f^{(3)}_{|000\rangle_{\mathrm{TLR}}\otimes|011\rangle_q},$$
$$\langle b_1^\dagger b_1\rangle = \left|f^{(2,3)}_{|010\rangle_{\mathrm{TLR}}\otimes|100\rangle_q}\right|^2 + \left|f^{(3)}_{|000\rangle_{\mathrm{TLR}}\otimes|110\rangle_q}\right|^2 + \left|f^{(3)}_{|021\rangle_{\mathrm{TLR}}\otimes|100\rangle_q}\right|^2 + \left|f^{(3)}_{|120\rangle_{\mathrm{TLR}}\otimes|100\rangle_q}\right|^2,$$
$$\langle b_3^\dagger b_3\rangle = \left|f^{(2,3)}_{|010\rangle_{\mathrm{TLR}}\otimes|001\rangle_q}\right|^2 + \left|f^{(3)}_{|000\rangle_{\mathrm{TLR}}\otimes|011\rangle_q}\right|^2 + \left|f^{(3)}_{|021\rangle_{\mathrm{TLR}}\otimes|001\rangle_q}\right|^2 + \left|f^{(3)}_{|120\rangle_{\mathrm{TLR}}\otimes|001\rangle_q}\right|^2,$$
$$\langle b_2^\dagger b_2\rangle = \left|f^{(3)}_{|000\rangle_{\mathrm{TLR}}\otimes|110\rangle_q}\right|^2 + \left|f^{(3)}_{|000\rangle_{\mathrm{TLR}}\otimes|011\rangle_q}\right|^2 + \left|f^{(3)}_{|012\rangle_{\mathrm{TLR}}\otimes|010\rangle_q}\right|^2 + \left|f^{(3)}_{|210\rangle_{\mathrm{TLR}}\otimes|010\rangle_q}\right|^2 + \left|f^{(3)}_{|111\rangle_{\mathrm{TLR}}\otimes|010\rangle_q}\right|^2 + \left|f^{(2,3)}_{|001\rangle_{\mathrm{TLR}}\otimes|010\rangle_q}\right|^2 + \left|f^{(2,3)}_{|100\rangle_{\mathrm{TLR}}\otimes|010\rangle_q}\right|^2, \tag{6}$$

where f is the perturbative coefficient of $|\Phi(t)\rangle$, and the superscripts represent the orders in the perturbative expression at which the f appears. The expression of f is shown in the Appendix.

B. Criteria for the multipartite EPR steering

EPR steering criteria [33] proposed by Reid are typically used to study the EPR steering, and we will employ the criteria to our system. Defining two quadrature operators as $X_{d_k} = d_k + d_k^\dagger$, $Y_{d_k} = -i(d_k - d_k^\dagger)$, $d_k = a_k, b_k$. The EPR steering criteria are given by [33,36]

$$W_{d_l\to d_k} = V_{\mathrm{inf}}(X_{d_k})V_{\mathrm{inf}}(Y_{d_k}) < 1\ (d_l \to d_k) \tag{7}$$

or

$$W_{d_k\to d_l} = V_{\mathrm{inf}}(X_{d_l})V_{\mathrm{inf}}(Y_{d_l}) < 1\ (d_k \to d_l), \tag{8}$$

and the variances mentioned are defined as

$$V_{\mathrm{inf}}(X_{d_k(d_l)}) = V(X_{d_k(d_l)}) - \frac{V^2(X_{d_k}, X_{d_l})}{V(X_{d_l(d_k)})}, \tag{9}$$

$k, l = 1, 2, 3,\ \ k \neq l$, and $V(n) = \langle n^2\rangle - \langle n\rangle^2$, $V(n,m) = \langle nm\rangle - \langle n\rangle\langle m\rangle$. In our system, $\langle d_k^2\rangle = 0$ and $\langle d_k d_l^\dagger\rangle = 0$ [49,50]; we employ witness to determine whether the EPR steering occurs:

$$w_{d_l\to d_k} = \frac{\langle d_k^\dagger d_k\rangle\left(\langle d_l^\dagger d_l\rangle + \frac{1}{2}\right)}{|\langle d_k d_l\rangle|^2} < 1, \tag{10}$$
$$w_{d_k\to d_l} = \frac{\langle d_l^\dagger d_l\rangle\left(\langle d_k^\dagger d_k\rangle + \frac{1}{2}\right)}{|\langle d_l d_k\rangle|^2} < 1. \tag{11}$$

The condition $w_{d_l\to d_k} < 1$ ($w_{d_k\to d_l} < 1$) proves the one-way EPR steering for $d_l \to d_k$ ($d_k \to d_l$). The one-way EPR steering occurs when one of them holds. If inequality (10) and inequality (11) hold simultaneously, there will be two-way EPR steering for $d_l \leftrightarrow d_k$.

C. Multipartite EPR steering in the DCA

In this section, we focus on the multipartite EPR steering. The EPR steering for RLC resonator modes vary with time in Fig. 2. Due to the DCE, there are pairs of Casimir photons created in the system. The state of field will be influenced by photon generation and increases with time, which results in sudden death for the EPR steering in the system [51]. Figure 2 also exhibits disappearance orders of the EPR steering for different modes. At first, there are two pairs of two-way EPR steerings for $b_1 \leftrightarrow b_2$ and $b_2 \leftrightarrow b_3$; these EPR steering correlations have disappeared successively over time in Figs. 2(a) and 2(b), and corresponding disappearance orders represented by different colors and types of arrows are described in Fig. 2(d). We can clearly see that the EPR steering for $b_2 \to b_1$ shows the strongest robustness against the time. The time-dependent external driving flux $\phi_{ext}(t)$ of SQUID can be considered as a switch, and the different types of the EPR steering will be obtained through operating the switch in the system. In Fig. 2, turning off the ϕ_{ext} at $t = 0.07$ or (0.11) ns, EPR steering decoherence source caused by the DCE will be cut off, and the system remain desired two-way EPR steering for $b_2 \leftrightarrow b_1$ or one-way EPR steering for $b_2 \to b_1$, respectively. We have realized the multipartite EPR steerings' orderly sudden death in Fig. 2, and the system is convenient for turning on or off the external flux of SQUID to control the state of the system. These characteristics are conducive to different quantum researches, such as quantum secret sharing [52]. If we change TLR frequencies, such as $\Omega_1/2\pi = 5$ GHZ, $\Omega_2/2\pi = 4$ GHZ, and $\Omega_3/2\pi = 6$ GHZ, the disappeared orders are different and the EPR steering for $b_3 \to b_2$ shows the strongest robustness against the time (not shown here). The superconducting circuit used in the model has excellent controllability, and it is convenient to turn on or off the external driving flux ϕ_{ext} and control TLR frequencies in the system. Now we take the time as a constant and study the effect of other parameters on EPR steering. Figure 3(a) shows that b_2 can steer b_1 but b_1 cannot steer

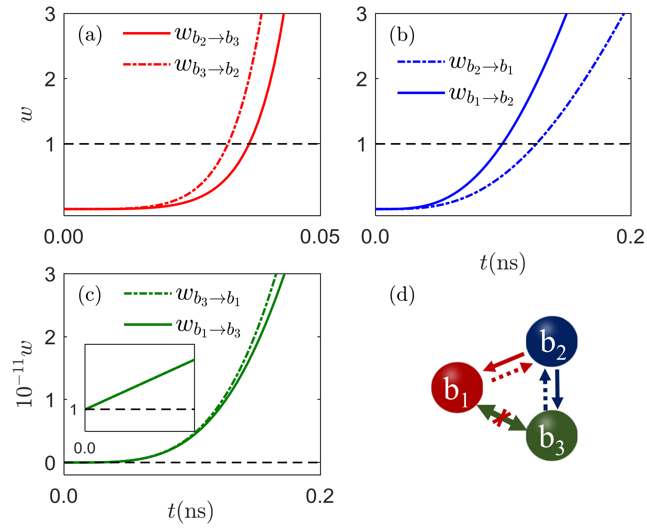

FIG. 2. Time evolution of witnesses $w_{b_k\to b_l}$ in (a)–(c). In (d), the red, blue, and green circles represent RLC resonator modes b_1, b_2, and b_3, respectively. The green solid arrow (with red crosses) represents no EPR steering, and the blue arrows disappear earlier than the red ones. As for the same color arrows, the dashed arrow disappears earlier than the solid arrow. The related parameters are $\Omega_1/2\pi = 3.2$ GHZ, $\Omega_2/2\pi = 4.8$ GHZ, and $\Omega_3/2\pi = 7$ GHZ for the three TLRs. The TLR-TLR coupling strengths are $\beta_0^{1,2} = \beta_0^{2,3} = \beta_0^{1,3} = 0.005\Omega_1$. Each RLC resonator resonantly interacts with corresponding TLR with the coupling strength $G_k = 0.04\Omega_2$ ($k = 1, 2, 3$).

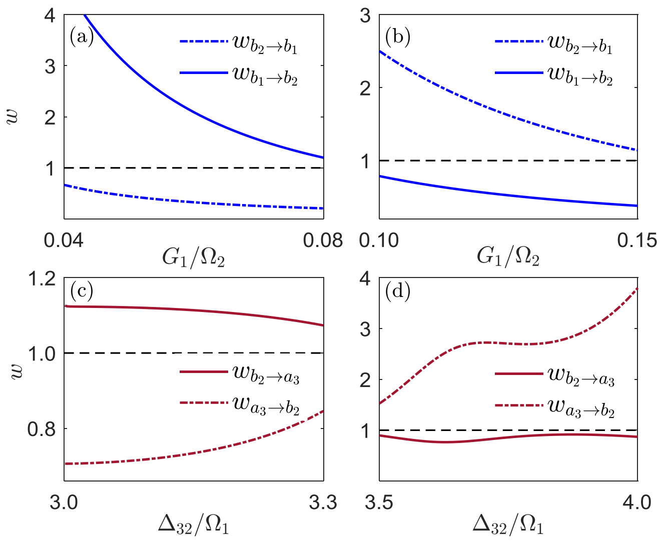

FIG. 3. $w_{b_2\to b_1}$ and $w_{b_1\to b_2}$ vary with G_1/Ω_2 under the condition of $G_2/G_1 = 2$ in (a), $G_2/G_1 = 0.4$ in (b). In (a) and (b), parameters we choose are $\Omega_1/2\pi = 3.2$ GHZ, $\Omega_2/2\pi = 4.8$ GHZ, and $\Omega_3/2\pi = 7$ GHZ, $t = 0.18$ ns, $G_3 = 0.04\Omega_2$, $\beta_0^{1,2} = \beta_0^{2,3} = \beta_0^{1,3} = 0.005\Omega_1$. $w_{a_3\to b_2}$ and $w_{b_2\to a_3}$ vary with detuning Δ_{32}/Ω_1 in (c) and (d), other parameters we choose are $\Omega_1/2\pi = 3.2$ GHZ, $\Omega_2/2\pi = 4.8$ GHZ, $t = 0.6$ ns, $G_1 = G_3 = 0.6G_2 = 0.04\Omega_2$, $\beta_0^{1,2} = \beta_0^{2,3} = \beta_0^{1,3} = 0.005\Omega_1$.

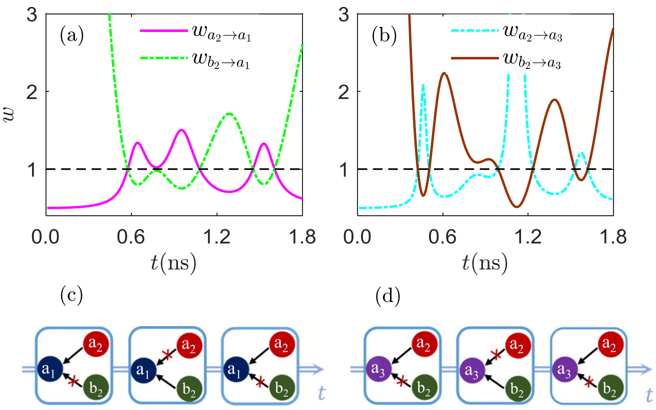

FIG. 4. Time evolution of $w_{a_2\to a_1}$ and $w_{b_2\to a_1}$ in (a), $w_{a_2\to a_3}$ and $w_{b_2\to a_3}$ in (b). The corresponding parameters are the same as Fig. 2.

b_2 simultaneously with $G_2/G_1 = 2$. On the contrary, we have made $G_2/G_1 = 0.4$ in Fig. 3(b) and the one-way EPR steering for $b_1 \to b_2$ occurs. According to the Figs. 3(a) and 3(b), if G_1 is relatively smaller than G_2, it is easier to realize the EPR steering for $b_2 \to b_1$ and the reverse is true. That is, we can reverse the direction of one-way EPR steering via controllable parameter (G_2/G_1) inversion in the system. In addition, Figs. 3(c) and 3(d) realize the one-way EPR steering for $a_3 \to b_2$ or $b_2 \to a_3$ in terms of controlling different detuning (Δ_{32}) region. The direction of one-way EPR steering can also be reversed via tuning parameter (Δ_{32}). In summary, our superconducting waveguide system has the advantage of being simple for controlling parameters, which is conducive to reverse the direction of the one-way EPR steering.

The preceding parts show a detailed discussion about the EPR steering. The system not only realizes the EPR steerings' orderly sudden death, but also reverses the direction of the EPR steering by tuning parameters. The multipartite EPR steering is useful for the quantum information transmission [53], provides a suitable way to realize quantun secure communication [54], and lays a foundation for constructing more complex quantum networks [54]. Tunable external driving flux ϕ_{ext} plays an important role in the system, turning it off at reasonable time to get desired state of the system. We can obtain completely different results compared with Fig. 2, and realize the controllability of the quantum state with the adjustment of TLR frequencies.

D. Monogamy relations in the DCA

We have discussed the multipartite EPR steering for different modes and found some interesting phenomena in Sec. III C. In this section, we focus on the monogamy relations of multipartite EPR steering, which play an important role in quantum information transmission. He *et al.* have studied four diverse types of monogamy relations based on the cascaded FWM [29]. Here, we propose coupled TLR and RLC resonators in the DCA to investigate monogamy relations of multipartite EPR steering.

We note the first photon-RLC resonator interaction term in Hamiltonian (5), $\hbar\sum_{k=1}^{3} G_k(b_k^\dagger a_k + b_k a_k^\dagger)$, which can be used to swap states between photon modes and resonator modes. Therefore, the model can realize quantum information swapping between different modes, as shown in Fig. 4. In Fig. 4(a), the EPR steering for $a_2 \to a_1$ occurs during the region of $0 < t(\text{ns}) < 0.58$, b_2 cannot steer a_1 at the same time. The phenomenon belongs to the type-I monogamy relation [29]; two diverse modes cannot steer the same third one simultaneously. However, when $0.58 < t(\text{ns}) < 1.1$, the EPR steering for $a_2 \to a_1$ disappears and b_2 begin to steer a_1, which is the type-I monogamy relation of $b_2 \to a_1$. As for a same steered party a_1, the above process can be understood as the conversion of steering party from $a_2 \Rightarrow b_2$, and the system achieves the type-I monogamy relation swapping. As shown in Fig. 4(a), there is continuous swapping between steering parties of the type-I monogamy relation over time. In Fig. 4(b), as for a same steered party a_3, the system realizes the type-I monogamy relation swapping for $(a_2 \to a_3) \Leftrightarrow (b_2 \to a_3)$ ($\Leftrightarrow$ represents monogamy relation swapping, $\to$ represents the EPR steering) due to steering party conversion between a_2 and b_2, switching off the external driving flux in reasonable time to obtain desired monogamy relation. If changing TLR frequencies, such as $\Omega_1/2\pi = 5$ GHZ, $\Omega_2/2\pi = 4$ GHZ, and $\Omega_3/2\pi = 6$ GHZ, we can realize the monogamy relation swapping in terms of the steering party conversion between a_3 and b_3 (not shown here).

Now we take the time as a constant and study the effect of other parameters on monogamy relation. We focus on the three-mode combination in Fig. 5. This is shown in Fig. 5(a), where b_2 as steered party, b_1 can steer it but b_3 cannot simultaneously. This is the type-I monogamy relation of $b_1 \to b_2$, corresponding monogamy relation is shown in Fig. 5(c). Compared with Fig. 5(a), we change the detuning Δ_{32} and get the type-I monogamy relation of $b_3 \to b_2$ in Fig. 5(b); the

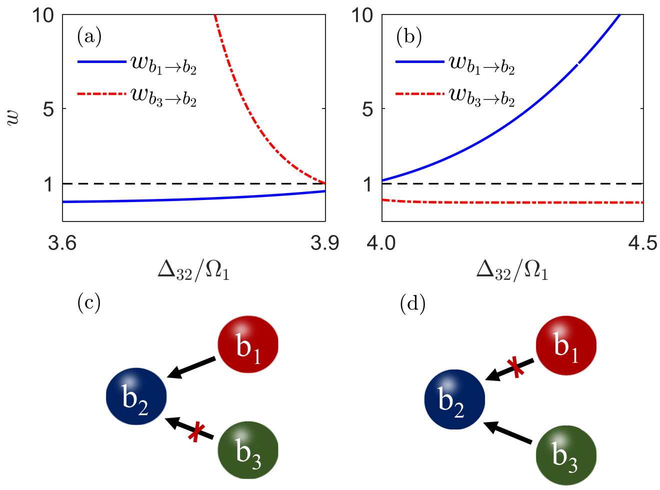

FIG. 5. $w_{b_1\to b_2}$ and $w_{b_3\to b_2}$ as function of detuning Δ_{32}/Ω_1 in (a) and (b). Corresponding type-I monogamy relations are shown in (c) and (d). Other parameters are $\Omega_1/2\pi = 3.2$ GHZ, $\Omega_3/2\pi = 7$ GHZ, $t = 0.06$ ns, $G_1 = 1.5G_2 = G_3 = 0.09\Omega_1$, $\beta_0^{1,2} = \beta_0^{2,3} = \beta_0^{1,3} = 0.005\Omega_1$.

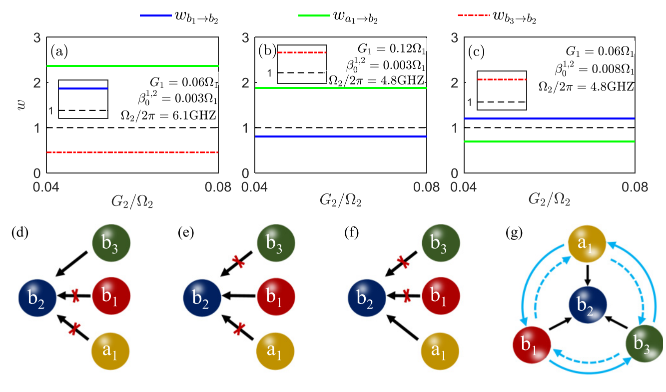

FIG. 7. $w_{a_1\to b_2}$, $w_{b_1\to b_2}$, and $w_{b_3\to b_2}$ vary with G_2/Ω_2 under the condition of $G_1 = 0.06\Omega_1$, $\beta_0^{1,2} = 0.003\Omega_1$, $\Omega_2/2\pi = 6.1$ GHZ in (a), $G_1 = 0.12\Omega_1$, $\beta_0^{1,2} = 0.003\Omega_1$, $\Omega_2/2\pi = 4.8$ GHZ in (b), $G_1 = 0.06\Omega_1$, $\beta_0^{1,2} = 0.008\Omega_1$, $\Omega_2/2\pi = 4.8$ GHZ in (c). Each figure plots the witness with the same region of G_2/Ω_2 in (a)–(c). Corresponding type-I monogamy relations described in (d)–(f) and monogamy relation cycling shown in (g). Other parameters are $\Omega_1/2\pi = 3.2$ GHZ, $\Omega_3/2\pi = 7$ GHZ, $G_3 = 0.12\Omega_1$, $t = 0.06$ ns, $\beta_0^{2,3} = \beta_0^{1,3} = 0.005\Omega_1$.

corresponding monogamy relation is shown in Fig. 5(d). The steering party can be converted between b_1 and b_3 by tuning detuning Δ_{32} to obtain a type-I monogamy relation swapping in the system.

Figure 6 shows another two three-mode combinations. a_1 can steer b_2 during the region of $1.09 < \Delta_{12}/\Omega_3 < 1.66$ in Fig. 6(a), but a_3 cannot steer b_2 in the same region in Fig. 6(b), which indicates the type-I monogamy relation of $a_1 \to b_2$. However, if tuning parameter Δ_{12}, the type-I monogamy relation of $a_1 \to b_2$ can be lifted and we will realize the type-I monogamy relation of $a_3 \to b_2$ for the case of $1 < \Delta_{12}/\Omega_3 < 1.05$ or $1.7 < \Delta_{12}/\Omega_3 < 1.8$ in Figs. 6(a) and 6(b). As for a same steered party b_2, the system realizes the steering party swapping between a_1 and a_3, which can be regarded as the monogamy relation swapping. Similarly, the system also realizes the monogamy relation of $a_1 \to a_2$ or $a_3 \to a_2$ and obtains corresponding monogamy relation swapping in Figs. 6(c) and 6(d). The above discussion confirms that

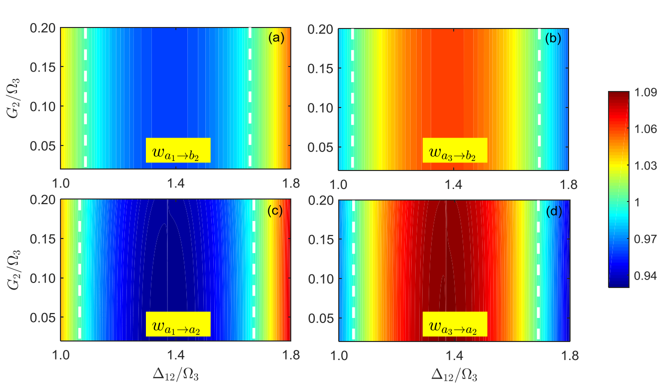

FIG. 6. $w_{a_1\to b_2}$, $w_{a_3\to b_2}$, $w_{a_1\to a_2}$, and $w_{a_3\to a_2}$ as functions of detuning Δ_{12}/Ω_3 and coupling strength G_2/Ω_3 in (a)–(d), respectively. Other parameters are $\Omega_2/2\pi = 4.8$ GHZ, $\Omega_3/2\pi = 7$ GHZ, $t = 0.1$ ns, $G_1 = G_3 = 0.04\Omega_2$, $\beta_0^{1,2} = \beta_0^{2,3} = \beta_0^{1,3} = 0.032\pi$ GHZ.

the steering party can be converted between a_1 and a_3 in terms of tuning detuning Δ_{12} to obtain type-I monogamy relation swapping. Comparing Fig. 6(a) with Fig. 6(c), the mode a_1 can steer b_2 and a_2 with same parameter range when $1.09 < \Delta_{12}/\Omega_3 < 1.66$. This is shown in Figs. 6(b) and 6(d), a_3, as steering party, can also steer b_2 and a_2 when $1 < \Delta_{12}/\Omega_3 < 1.05$ or $1.7 < \Delta_{12}/\Omega_3 < 1.8$. In addition to realizing type-I monogamy relation swapping by converting steering parties between a_1 and a_3, the steering party (a_1 or a_3) can also steer two steered parties (b_2 and a_2) simultaneously.

Figure 7 discusses the four-mode combination in which b_2 as steered party, and b_1, b_3, and a_1 as steering parties. It is clear that only the $w_{b_3\to b_2} < 1$ in Fig. 7(a), which indicates the type-I monogamy relation of $b_3 \to b_2$ depicted in Fig. 7(d). In addition, Fig. 7(a) exhibits the robustness of the EPR steering for $b_3 \to b_2$ against the coupling. Compared with Fig. 7(a), we tune the parameters G_1 and Ω_2 in Fig. 7(b) and parameters Ω_2 and $\beta_0^{1,2}$ by adjusting the external flux of SQUID in Fig. 7(c). The type-I monogamy relation of $b_3 \to b_2$ is lifted, and the type-I monogamy relations of $b_1 \to b_2$ and $a_1 \to b_2$ are obtained, respectively. The steering party cycling for $b_3 \Rightarrow b_1 \Rightarrow a_1 \Rightarrow b_3$ is realized in terms of controlling parameters, which can be understood as the monogamy relation cycling for $(b_3 \to b_2) \Rightarrow (b_1 \to b_2) \Rightarrow (a_1 \to b_2) \Rightarrow (b_3 \to b_2)$ ($\Rightarrow$ represents monogamy relation cycling, $\to$ represents the EPR steering), as shown in Fig. 7(g). The system also realizes the robustness of the EPR steering for $b_1 \to b_2$ and $a_1 \to b_2$ against the coupling in Figs. 7(b) and 7(c), respectively. Similarly, we also realize the monogamy relation cycling in the opposite direction via tuning parameters G_1, Ω_2, and $\beta_0^{1,2}$ in Fig. 7(g). In a word, the steering party can be converted in the order of blue arrows in Fig. 7(g), which is the type-I monogamy relation cycling. It is similar to the three-mode combinations, and the controllable type-I monogamy relation

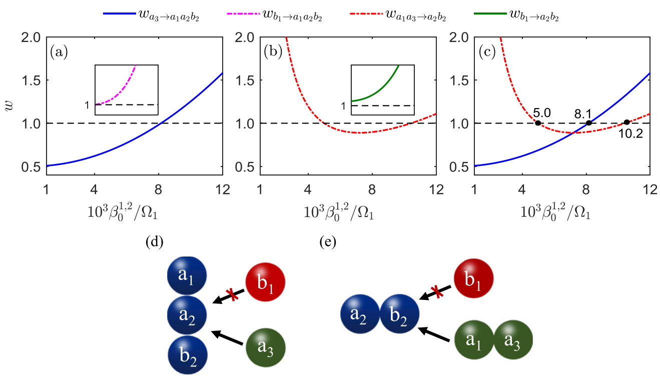

FIG. 8. $w_{a_3\to a_1a_2b_2}$, $w_{b_1\to a_1a_2b_2}$, $w_{a_1a_3\to a_2b_2}$, and $w_{b_1\to a_2b_2}$ vary with $\beta_0^{1,2}/\Omega_1$ under the condition of $t = 2.55$ ns in (a)–(c). Each figure plots the witness with same region of $\beta_0^{1,2}/\Omega_1$ in (a)–(c). Corresponding type-II monogamy relations are shown in (d) and (e). Other parameters are $\Omega_1/2\pi = 3.2$ GHZ, $\Omega_2/2\pi = 4.8$ GHZ, $\Omega_3/2\pi = 7$ GHZ, $G_1 = G_2 = G_3 = 0.04\Omega_2$, $\beta_0^{2,3} = \beta_0^{1,3} = 0.005\Omega_1$.

has been realized through tunable parameters in four-mode combination in the system.

Finally, we begin with the five-mode combination containing a_1, a_2, a_3, b_1, b_2 and investigate corresponding monogamy relations of the multipartite EPR steering. In Fig. 8(a), there is the EPR steering for $a_3 \to a_1a_2b_2$, but b_1 cannot steer the group $(a_1a_2b_2)$ during the region of $1 \leqslant \beta_0^{1,2}/\Omega_1(\times 10^{-3}) \leqslant 8.1$. In Fig. 8(b), the group (a_1a_3) can steer the group (a_2b_2), but the mode b_1 cannot steer the group (a_2b_2) under the condition of $5 \leqslant \beta_0^{1,2}/\Omega_1(\times 10^{-3}) \leqslant 10.2$. The above EPR steerings have the common characteristic, that is, the steered parties consist of more than one mode and can only be steered by one independent group, which belongs to the type-II monogamy relation [29]. Comparing Figs. 8(a) and 8(b), we find that the two type-II monogamy relations hold in different parameter regions. The type-II monogamy relation of $a_3 \to a_1a_2b_2$ is obtained and the type-II monogamy relation of $a_1a_3 \to a_2b_2$ is lifted when $1.0 < \beta_0^{1,2}/\Omega_1(\times 10^{-3}) < 5.0$. However, during the region of $8.1 < \beta_0^{1,2}/\Omega_1(\times 10^{-3}) < 10.2$, the type-II monogamy relation of $a_3 \to a_1a_2b_2$ is lifted and the type-II monogamy relation of $a_1a_3 \to a_2b_2$ is realized. The above process can be regarded as the monogamy relation swapping. The steering party can be converted between the mode a_3 and the group (a_1a_3) to obtain the type-II monogamy relation swapping with the adjustment of parameter $\beta_0^{1,2}$, where controllable $\beta_0^{1,2}$ can be obtained through tuning flux ϕ_{ext} of SQUID. In addition to realizing type-II monogamy relation of the multipartite EPR steering, the system can also convert steering party to obtain type-II monogamy relation swapping.

It is innovative to discuss the monogamy relations in the frame of superconducting circuit based on the DCE, which is different from the paper [28,29]. We can get type-I and type-II monogamy relation swapping and cycling by converting steering parties with the adjustment of corresponding parameters in such a conveniently manipulative superconducting circuit.

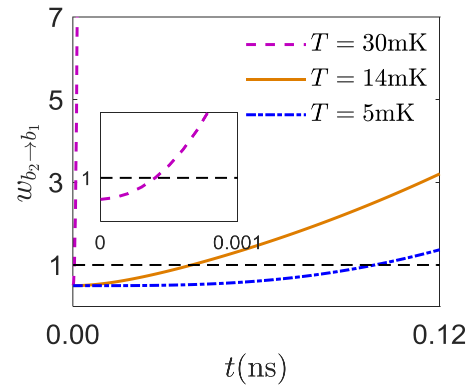

FIG. 9. Witnesses $w_{b_2\to b_1}$ vary with time with different temperatures. Other parameters are the same as Fig. 2.

E. Influence of temperature on the system

In superconducting circuit experiments, the environment temperature must be taken into account. Therefore, we discuss the influence of temperature in this section. For the sake of simplicity, we only consider the temperature of the TLR_1. The initial state of the system becomes $|n_1 00\rangle_{\text{TLR}} \otimes |000\rangle_q$, where $n_1 = (e^{\frac{\hbar\Omega_1}{kT}} - 1)^{-1}$. Figure 9 plots the witness $b_2 \to b_1$ varying with time at different temperatures. The higher the temperature is, the earlier sudden death for the EPR steering is. The low temperature is beneficial to the existence of the EPR steering. Figure 10 shows time evolution of the EPR steering for RLC resonator modes when the system contains a reasonable amount of measurement noise. Compared with Fig. 2, there are the same disappearance orders of the EPR steering in Fig. 10, but corresponding sudden death for the EPR steering is faster. For example, there is the sudden death for the EPR steering of $b_2 \to b_1$ when $t = 0.13$ ns in Fig. 2 and $t = 0.10$ ns in Fig. 10. Therefore, reducing measurement noise is necessary for quantum information operation and transmission.

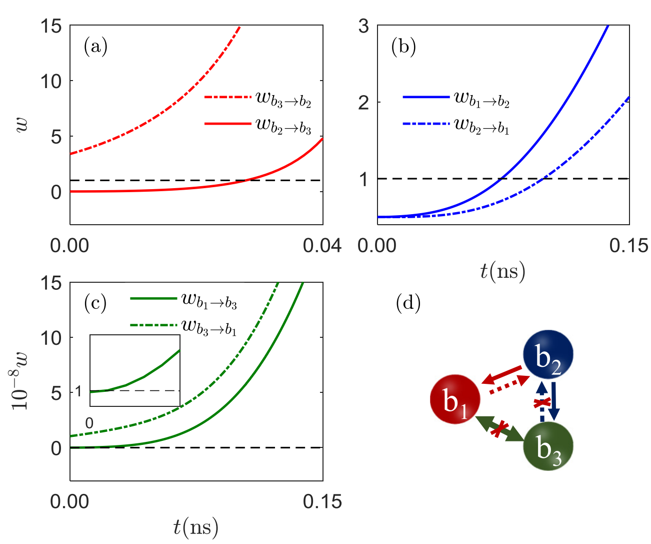

FIG. 10. Time evolution of witnesses $w_{b_k\to b_l}$ in (a)–(c). In (d), different colors and types of arrows represent disappearance orders; more details refer to Fig. 2 caption. The related temperature is $T = 4$ mK, and other parameters are the same as Fig. 2.

IV. CONCLUSION

In conclusion, we have studied the multipartite EPR steering and type-I and type-II monogamy relations by means of the DCE in the frame of conveniently manipulative superconducting waveguide circuit. We get the following results through analysis and calculation.

The external driving flux of the SQUID plays an important role in the system, and we can control the EPR steering and monogamy relations by switching on or off the flux. The system has achieved the one-way or two-way EPR steering generation and orderly sudden death for RLC resonator modes, and reversing the direction of the one-way EPR steering with the adjustment of coupling parameters. Furthermore, the type-I and type-II monogamy relations have been obtained in the system, and we also get monogamy relations swapping and cycling via converting steering parties in suitable parameter ranges of detunings or coupling strengths. A proposed circuit cannot avoid measurement noise. We find that low temperature is conducive to the existence of the EPR steering.

We implement an innovative way to investigate the monogamy relations of the multipartite EPR steering, in the DCA under the framework of superconducting quantum circuit. In summary, based on all the above conclusions, the paper is conducive to the research and development of quantum information, provides a suitable way for the secure quantum communication, and lays a foundation for constructing more complex quantum networks.

ACKNOWLEDGMENT

This work is supported by National Natural Science Foundation of China (NSFC) (Grants No. 11175044 and No. 11347190).

APPENDIX

We exhibit some average values $\langle d_k d_l\rangle$ and $\langle d_k^\dagger d_k\rangle$ in Sec. III A, and the rest of the values are expressed as follows:

$$
\begin{aligned}
\langle a_1 b_2\rangle &= f^{(0,2,3)*}_{|000\rangle_{\rm TLR}\otimes|000\rangle_q} f^{(2,3)}_{|100\rangle_{\rm TLR}\otimes|010\rangle_q} + \sqrt{2} f^{(1,2,3)*}_{|110\rangle_{\rm TLR}\otimes|000\rangle_q} f^{(3)}_{|210\rangle_{\rm TLR}\otimes|010\rangle_q} + f^{(1,2,3)*}_{|011\rangle_{\rm TLR}\otimes|000\rangle_q} f^{(3)}_{|111\rangle_{\rm TLR}\otimes|010\rangle_q},\\
\langle b_2 a_1\rangle &= f^{(0,2,3)*}_{|000\rangle_{\rm TLR}\otimes|000\rangle_q} f^{(2,3)}_{|100\rangle_{\rm TLR}\otimes|010\rangle_q} + \sqrt{2} f^{(1,2,3)*}_{|110\rangle_{\rm TLR}\otimes|000\rangle_q} f^{(3)}_{|210\rangle_{\rm TLR}\otimes|010\rangle_q} + f^{(1,2,3)*}_{|011\rangle_{\rm TLR}\otimes|000\rangle_q} f^{(3)}_{|111\rangle_{\rm TLR}\otimes|010\rangle_q},\\
\langle a_3 b_2\rangle &= f^{(0,2,3)*}_{|000\rangle_{\rm TLR}\otimes|000\rangle_q} f^{(2,3)}_{|001\rangle_{\rm TLR}\otimes|010\rangle_q} + \sqrt{2} f^{(1,2,3)*}_{|011\rangle_{\rm TLR}\otimes|000\rangle_q} f^{(3)}_{|012\rangle_{\rm TLR}\otimes|010\rangle_q} + f^{(1,2,3)*}_{|011\rangle_{\rm TLR}\otimes|000\rangle_q} f^{(3)}_{|111\rangle_{\rm TLR}\otimes|010\rangle_q},\\
\langle b_2 a_3\rangle &= f^{(0,2,3)*}_{|000\rangle_{\rm TLR}\otimes|000\rangle_q} f^{(2,3)}_{|001\rangle_{\rm TLR}\otimes|010\rangle_q} + \sqrt{2} f^{(1,2,3)*}_{|011\rangle_{\rm TLR}\otimes|000\rangle_q} f^{(3)}_{|012\rangle_{\rm TLR}\otimes|010\rangle_q} + f^{(1,2,3)*}_{|011\rangle_{\rm TLR}\otimes|000\rangle_q} f^{(3)}_{|111\rangle_{\rm TLR}\otimes|010\rangle_q},\\
\langle a_1 a_2\rangle &= f^{(0,2,3)*}_{|000\rangle_{\rm TLR}\otimes|000\rangle_q} f^{(1,2,3)}_{|110\rangle_{\rm TLR}\otimes|000\rangle_q} + f^{(2,3)*}_{|001\rangle_{\rm TLR}\otimes|010\rangle_q} f^{(3)}_{|111\rangle_{\rm TLR}\otimes|010\rangle_q} + \sqrt{3} f^{(2,3)*}_{|022\rangle_{\rm TLR}\otimes|000\rangle_q} f^{(3)}_{|132\rangle_{\rm TLR}\otimes|000\rangle_q}\\
&\quad + \sqrt{6} f^{(2,3)*}_{|121\rangle_{\rm TLR}\otimes|000\rangle_q} f^{(3)}_{|231\rangle_{\rm TLR}\otimes|000\rangle_q} + 2 f^{(1,2,3)*}_{|110\rangle_{\rm TLR}\otimes|000\rangle_q} f^{(2,3)}_{|220\rangle_{\rm TLR}\otimes|000\rangle_q} + 3 f^{(2,3)*}_{|220\rangle_{\rm TLR}\otimes|000\rangle_q} f^{(3)}_{|330\rangle_{\rm TLR}\otimes|000\rangle_q}\\
&\quad + \sqrt{2}\big(f^{(1,2,3)*}_{|011\rangle_{\rm TLR}\otimes|000\rangle_q} f^{(2,3)}_{|121\rangle_{\rm TLR}\otimes|000\rangle_q} + f^{(2,3)*}_{|100\rangle_{\rm TLR}\otimes|010\rangle_q} f^{(2,3)}_{|210\rangle_{\rm TLR}\otimes|010\rangle_q} + f^{(2,3)*}_{|010\rangle_{\rm TLR}\otimes|001\rangle_q} f^{(2,3)}_{|120\rangle_{\rm TLR}\otimes|001\rangle_q}\\
&\quad + f^{(2,3)*}_{|010\rangle_{\rm TLR}\otimes|100\rangle_q} f^{(3)}_{|120\rangle_{\rm TLR}\otimes|100\rangle_q}\big),\\
\langle a_2 a_1\rangle &= f^{(0,2,3)*}_{|000\rangle_{\rm TLR}\otimes|000\rangle_q} f^{(1,2,3)}_{|110\rangle_{\rm TLR}\otimes|000\rangle_q} + f^{(2,3)*}_{|001\rangle_{\rm TLR}\otimes|010\rangle_q} f^{(3)}_{|111\rangle_{\rm TLR}\otimes|010\rangle_q} + \sqrt{3} f^{(2,3)*}_{|022\rangle_{\rm TLR}\otimes|000\rangle_q} f^{(3)}_{|132\rangle_{\rm TLR}\otimes|000\rangle_q}\\
&\quad + \sqrt{6} f^{(2,3)*}_{|121\rangle_{\rm TLR}\otimes|000\rangle_q} f^{(3)}_{|231\rangle_{\rm TLR}\otimes|000\rangle_q} + 2 f^{(1,2,3)*}_{|110\rangle_{\rm TLR}\otimes|000\rangle_q} f^{(2,3)}_{|220\rangle_{\rm TLR}\otimes|000\rangle_q} + 3 f^{(2,3)*}_{|220\rangle_{\rm TLR}\otimes|000\rangle_q} f^{(3)}_{|330\rangle_{\rm TLR}\otimes|000\rangle_q}\\
&\quad + \sqrt{2}\big(f^{(1,2,3)*}_{|011\rangle_{\rm TLR}\otimes|000\rangle_q} f^{(2,3)}_{|121\rangle_{\rm TLR}\otimes|000\rangle_q} + f^{(2,3)*}_{|100\rangle_{\rm TLR}\otimes|010\rangle_q} f^{(2,3)}_{|210\rangle_{\rm TLR}\otimes|010\rangle_q} + f^{(2,3)*}_{|010\rangle_{\rm TLR}\otimes|001\rangle_q} f^{(2,3)}_{|120\rangle_{\rm TLR}\otimes|001\rangle_q}\\
&\quad + f^{(2,3)*}_{|010\rangle_{\rm TLR}\otimes|100\rangle_q} f^{(3)}_{|120\rangle_{\rm TLR}\otimes|100\rangle_q}\big),\\
\langle a_3 a_2\rangle &= f^{(0,2,3)*}_{|000\rangle_{\rm TLR}\otimes|000\rangle_q} f^{(1,2,3)}_{|011\rangle_{\rm TLR}\otimes|000\rangle_q} + f^{(2,3)*}_{|100\rangle_{\rm TLR}\otimes|010\rangle_q} f^{(3)}_{|111\rangle_{\rm TLR}\otimes|010\rangle_q} + \sqrt{3} f^{(2,3)*}_{|220\rangle_{\rm TLR}\otimes|000\rangle_q} f^{(3)}_{|231\rangle_{\rm TLR}\otimes|000\rangle_q}\\
&\quad + \sqrt{6} f^{(2,3)*}_{|121\rangle_{\rm TLR}\otimes|000\rangle_q} f^{(3)}_{|132\rangle_{\rm TLR}\otimes|000\rangle_q} + 2 f^{(1,2,3)*}_{|011\rangle_{\rm TLR}\otimes|000\rangle_q} f^{(2,3)}_{|022\rangle_{\rm TLR}\otimes|000\rangle_q} + 3 f^{(2,3)*}_{|022\rangle_{\rm TLR}\otimes|000\rangle_q} f^{(3)}_{|033\rangle_{\rm TLR}\otimes|000\rangle_q}\\
&\quad + \sqrt{2}\big(f^{(1,2,3)*}_{|110\rangle_{\rm TLR}\otimes|000\rangle_q} f^{(2,3)}_{|121\rangle_{\rm TLR}\otimes|000\rangle_q} + f^{(2,3)*}_{|010\rangle_{\rm TLR}\otimes|100\rangle_q} f^{(2,3)}_{|021\rangle_{\rm TLR}\otimes|100\rangle_q} + f^{(2,3)*}_{|010\rangle_{\rm TLR}\otimes|001\rangle_q} f^{(2,3)}_{|021\rangle_{\rm TLR}\otimes|001\rangle_q}\\
&\quad + f^{(2,3)*}_{|001\rangle_{\rm rm\,TLR}\otimes|010\rangle_q} f^{(3)}_{|012\rangle_{\rm TLR}\otimes|010\rangle_q}\big),\\
\langle a_2 a_3\rangle &= f^{(0,2,3)*}_{|000\rangle_{\rm TLR}\otimes|000\rangle_q} f^{(1,2,3)}_{|011\rangle_{\rm TLR}\otimes|000\rangle_q} + f^{(2,3)*}_{|100\rangle_{\rm TLR}\otimes|010\rangle_q} f^{(3)}_{|111\rangle_{\rm TLR}\otimes|010\rangle_q} + \sqrt{3} f^{(2,3)*}_{|220\rangle_{\rm TLR}\otimes|000\rangle_q} f^{(3)}_{|231\rangle_{\rm TLR}\otimes|000\rangle_q}\\
&\quad + \sqrt{6} f^{(2,3)*}_{|121\rangle_{\rm TLR}\otimes|000\rangle_q} f^{(3)}_{|132\rangle_{\rm TLR}\otimes|000\rangle_q} + 2 f^{(1,2,3)*}_{|011\rangle_{\rm TLR}\otimes|000\rangle_q} f^{(2,3)}_{|022\rangle_{\rm TLR}\otimes|000\rangle_q} + 3 f^{(2,3)*}_{|022\rangle_{\rm TLR}\otimes|000\rangle_q} f^{(3)}_{|033\rangle_{\rm TLR}\otimes|000\rangle_q}\\
&\quad + \sqrt{2}\big(f^{(1,2,3)*}_{|110\rangle_{\rm TLR}\otimes|000\rangle_q} f^{(2,3)}_{|121\rangle_{\rm TLR}\otimes|000\rangle_q} + f^{(2,3)*}_{|010\rangle_{\rm TLR}\otimes|100\rangle_q} f^{(2,3)}_{|021\rangle_{\rm TLR}\otimes|100\rangle_q} + f^{(2,3)*}_{|010\rangle_{\rm TLR}\otimes|001\rangle_q} f^{(2,3)}_{|021\rangle_{\rm TLR}\otimes|001\rangle_q}\\
&\quad + f^{(2,3)*}_{|001\rangle_{\rm rm\,TLR}\otimes|010\rangle_q} f^{(3)}_{|012\rangle_{\rm TLR}\otimes|010\rangle_q}\big),
\end{aligned}
$$

$$
\begin{aligned}
\langle a_1^\dagger a_1\rangle =& \left|f^{(2,3)}_{|100\rangle_{\mathrm{TLR}}\otimes|010\rangle_q}\right|^2+\left|f^{(3)}_{|120\rangle_{\mathrm{TLR}}\otimes|100\rangle_q}\right|^2+\left|f^{(3)}_{|120\rangle_{\mathrm{TLR}}\otimes|001\rangle_q}\right|^2+\left|f^{(3)}_{|111\rangle_{\mathrm{TLR}}\otimes|010\rangle_q}\right|^2+\left|f^{(1,2,3)}_{|110\rangle_{\mathrm{TLR}}\otimes|000\rangle_q}\right|^2\\
&+\left|f^{(2,3)}_{|121\rangle_{\mathrm{TLR}}\otimes|000\rangle_q}\right|^2+\left|f^{(3)}_{|132\rangle_{\mathrm{TLR}}\otimes|000\rangle_q}\right|^2+2\Big(\left|f^{(3)}_{|210\rangle_{\mathrm{TLR}}\otimes|010\rangle_q}\right|^2+\left|f^{(2,3)}_{|220\rangle_{\mathrm{TLR}}\otimes|000\rangle_q}\right|^2+\left|f^{(3)}_{|231\rangle_{\mathrm{TLR}}\otimes|000\rangle_q}\right|^2\Big)\\
&+3\left|f^{(3)}_{|330\rangle_{\mathrm{TLR}}\otimes|000\rangle_q}\right|^2,\\
\langle a_3^\dagger a_3\rangle =& \left|f^{(2,3)}_{|001\rangle_{\mathrm{TLR}}\otimes|010\rangle_q}\right|^2+\left|f^{(3)}_{|021\rangle_{\mathrm{TLR}}\otimes|100\rangle_q}\right|^2+\left|f^{(3)}_{|021\rangle_{\mathrm{TLR}}\otimes|001\rangle_q}\right|^2+\left|f^{(3)}_{|111\rangle_{\mathrm{TLR}}\otimes|010\rangle_q}\right|^2+\left|f^{(1,2,3)}_{|011\rangle_{\mathrm{TLR}}\otimes|000\rangle_q}\right|^2,\\
&+\left|f^{(2,3)}_{|121\rangle_{\mathrm{TLR}}\otimes|000\rangle_q}\right|^2+\left|f^{(3)}_{|231\rangle_{\mathrm{TLR}}\otimes|000\rangle_q}\right|^2+2\Big(\left|f^{(3)}_{|012\rangle_{\mathrm{TLR}}\otimes|010\rangle_q}\right|^2+\left|f^{(2,3)}_{|022\rangle_{\mathrm{TLR}}\otimes|000\rangle_q}\right|^2+\left|f^{(3)}_{|132\rangle_{\mathrm{TLR}}\otimes|000\rangle_q}\right|^2\Big)\\
&+3\left|f^{(3)}_{|033\rangle_{\mathrm{TLR}}\otimes|000\rangle_q}\right|^2,\\
\langle a_2^\dagger a_2\rangle =& \left|f^{(2,3)}_{|010\rangle_{\mathrm{TLR}}\otimes|001\rangle_q}\right|^2+\left|f^{(2,3)}_{|010\rangle_{\mathrm{TLR}}\otimes|100\rangle_q}\right|^2+\left|f^{(3)}_{|012\rangle_{\mathrm{TLR}}\otimes|010\rangle_q}\right|^2+\left|f^{(3)}_{|210\rangle_{\mathrm{TLR}}\otimes|010\rangle_q}\right|^2+\left|f^{(3)}_{|111\rangle_{\mathrm{TLR}}\otimes|010\rangle_q}\right|^2\\
&+2\Big(\left|f^{(3)}_{|021\rangle_{\mathrm{TLR}}\otimes|100\rangle_q}\right|^2+\left|f^{(3)}_{|021\rangle_{\mathrm{TLR}}\otimes|001\rangle_q}\right|^2+\left|f^{(3)}_{|120\rangle_{\mathrm{TLR}}\otimes|100\rangle_q}\right|^2+\left|f^{(3)}_{|120\rangle_{\mathrm{TLR}}\otimes|001\rangle_q}\right|^2+\left|f^{(2,3)}_{|220\rangle_{\mathrm{TLR}}\otimes|000\rangle_q}\right|^2\\
&+\left|f^{(2,3)}_{|022\rangle_{\mathrm{TLR}}\otimes|000\rangle_q}\right|^2+\left|f^{(2.3)}_{|121\rangle_{\mathrm{TLR}}\otimes|000\rangle_q}\right|^2\Big)+3\Big(\left|f^{(3)}_{|132\rangle_{\mathrm{TLR}}\otimes|000\rangle_q}\right|^2+\left|f^{(3)}_{|231\rangle_{\mathrm{TLR}}\otimes|000\rangle_q}\right|^2+\left|f^{(3)}_{|330\rangle_{\mathrm{TLR}}\otimes|000\rangle_q}\right|^2\\
&+\left|f^{(3)}_{|033\rangle_{\mathrm{TLR}}\otimes|000\rangle_q}\right|^2\Big)+\left|f^{(1,2,3)}_{|110\rangle_{\mathrm{TLR}}\otimes|000\rangle_q}\right|^2+\left|f^{(1,2,3)}_{|011\rangle_{\mathrm{TLR}}\otimes|000\rangle_q}\right|^2,
\end{aligned}
\tag{A1}
$$

$$
\begin{aligned}
\langle a_1^\dagger a_3^\dagger a_1 a_3\rangle =& \left|f^{(3)}_{|111\rangle_{\mathrm{TLR}}\otimes|010\rangle_q}\right|^2+\left|f^{(2,3)}_{|121\rangle_{\mathrm{TLR}}\otimes|000\rangle_q}\right|^2+2\Big(\left|f^{(3)}_{|132\rangle_{\mathrm{TLR}}\otimes|000\rangle_q}\right|^2+\left|f^{(3)}_{|231\rangle_{\mathrm{TLR}}\otimes|000\rangle_q}\right|^2\Big),\\
\langle a_2^\dagger b_2^\dagger a_2 b_2\rangle =& \left|f^{(3)}_{|111\rangle_{\mathrm{TLR}}\otimes|010\rangle_q}\right|^2+\left|f^{(3)}_{|210\rangle_{\mathrm{TLR}}\otimes|010\rangle_q}\right|^2+\left|f^{(3)}_{|012\rangle_{\mathrm{TLR}}\otimes|010\rangle_q}\right|^2,\quad \langle a_1a_2b_2b_1\rangle=\langle a_1a_2b_1\rangle=0,\\
\langle a_1^\dagger a_2^\dagger b_2^\dagger a_1 a_2 b_2\rangle =& \left|f^{(3)}_{|111\rangle_{\mathrm{TLR}}\otimes|010\rangle_q}\right|^2+2\left|f^{(3)}_{|210\rangle_{\mathrm{TLR}}\otimes|010\rangle_q}\right|^2,\quad \langle a_1a_2b_2a_3\rangle=\langle a_2b_2a_1a_3\rangle=f^{(0,2,3)*}_{|000\rangle_{\mathrm{TLR}}\otimes|000\rangle_q}f^{(3)}_{|111\rangle_{\mathrm{TLR}}\otimes|010\rangle_q}.
\end{aligned}
\tag{A2}
$$

The corresponding coefficients f expressed in Eqs. (6), (A1), and (A2) are expressed as follows:

$$
\begin{aligned}
f^{(3)}_{|021\rangle_{\mathrm{TLR}}\otimes|100\rangle_q} =& \frac{3\sqrt{2}\beta_0^{1,2}\beta_0^{2,3}G_1}{4a^2b}[(e^{iat}-iat-1)(1-e^{ibt})],\\
f^{(3)}_{|120\rangle_{\mathrm{TLR}}\otimes|001\rangle_q} =& \frac{3\sqrt{2}\beta_0^{1,2}\beta_0^{2,3}G_3}{4b^2a}[(e^{ibt}-ibt-1)(1-e^{iat})],\\
f^{(3)}_{|111\rangle_{\mathrm{TLR}}\otimes|010\rangle_q} =& \frac{\beta_0^{1,2}\beta_0^{2,3}G_2}{4a^2b^2}[(a+b)(1-e^{iat})(e^{ibt}-1)+abit(e^{iat}+e^{ibt}-2)],\\
f^{(2,3)}_{|010\rangle_{\mathrm{TLR}}\otimes|001\rangle_q} =& \frac{\beta_0^{1,2}\beta_0^{1,3}G_3}{4ac^2}(e^{-ict}+ict-1)+\frac{G_3}{4b^2}\big(2\beta_0^{2,3}-\beta_0^{1,2}\beta_0^{1,3}a^{-1}\big)(e^{ibt}-ibt-1),\\
f^{(2,3)}_{|010\rangle_{\mathrm{TLR}}\otimes|100\rangle_q} =& \frac{\beta_0^{2,3}\beta_0^{1,3}G_1}{4bc^2}(e^{-ict}+ict-1)+\frac{G_1}{4a^2}\big(2\beta_0^{1,2}-\beta_0^{2,3}\beta_0^{1,3}b^{-1}\big)(e^{iat}-iat-1),\\
f^{(2,3)}_{|100\rangle_{\mathrm{TLR}}\otimes|010\rangle_q} =& \frac{\beta_0^{1,2}G_2(e^{iat}-iat-1)}{2a^2}+\frac{\beta_0^{2,3}\beta_0^{1,3}G_2}{4b}\left[\left(\frac{1-e^{iat}+ibt}{ab}\right)-\frac{(1+ibt)(1-e^{ict})}{bc}+\frac{1-e^{iat}}{a^2}\right],\\
f^{(2,3)}_{|001\rangle_{\mathrm{TLR}}\otimes|010\rangle_q} =& \frac{\beta_0^{2,3}G_2(e^{ibt}-ibt-1)}{2b^2}+\frac{\beta_0^{1,2}\beta_0^{1,3}G_2}{4a}\left[\left(\frac{1-e^{ibt}+iat}{ab}\right)+\frac{(1+iat)(1-e^{-ict})}{ac}+\frac{1-e^{ibt}}{b^2}\right],\\
f^{(3)}_{|132\rangle_{\mathrm{TLR}}\otimes|000\rangle_q} =& \frac{\sqrt{3}\beta_0^{1,2}\beta_0^{2,3}\beta_0^{2,3}}{4b}\left(\frac{(a+3b)(1-e^{i(a+2b)t})}{2b(a+b)(a+2b)}+\frac{1-e^{iat}}{2ab}+\frac{e^{ibt}(e^{i(a+b)t}-1)}{a(a+b)}+\frac{e^{i(a+b)t}-1}{(a+b)b}\right)\\
&+\frac{\sqrt{3}\beta_0^{1,2}\beta_0^{2,3}\beta_0^{2,3}}{4a}\left(\frac{1-e^{i(a+2b)t}}{(a+b)(a+2b)}+\frac{e^{2ibt}-1}{2b^2}+\frac{e^{ibt}-1}{b(a+b)}+\frac{1-e^{ibt}}{b^2}\right),\\
f^{(3)}_{|231\rangle_{\mathrm{TLR}}\otimes|000\rangle_q} =& \frac{\sqrt{3}\beta_0^{1,2}\beta_0^{1,2}\beta_0^{2,3}}{4a}\left(\frac{(b+3a)(1-e^{i(b+2a)t})}{2a(a+b)(b+2a)}+\frac{1-e^{ibt}}{2ab}+\frac{e^{iat}(e^{i(a+b)t}-1)}{b(a+b)}+\frac{e^{i(a+b)t}-1}{a(a+b)}\right)\\
&+\frac{\sqrt{3}\beta_0^{1,2}\beta_0^{1,2}\beta_0^{2,3}}{4b}\left(\frac{1-e^{i(b+2a)t}}{(a+b)(b+2a)}+\frac{e^{2iat}-1}{2a^2}+\frac{e^{iat}-1}{a(a+b)}+\frac{1-e^{iat}}{a^2}\right),
\end{aligned}
$$

$$
\begin{aligned}
f^{(0,2,3)}_{|000\rangle_{\rm TLR}\otimes|000\rangle_q} &= 1 + \frac{\beta_0^{1,2}\beta_0^{2,3}\beta_0^{1,3}}{8}\left(\frac{(e^{-iat}-1)(b-c)}{a^2bc} + \frac{(1-e^{-ibt})(c+a)}{b^2ac} - \frac{e^{-ibt}-e^{-iat}}{abc} - \frac{2ti}{ab}\right)\\
&\quad + \frac{\beta_0^{1,2}\beta_0^{1,2}}{4a^2}(e^{-iat}-1+iat) + \frac{\beta_0^{2,3}\beta_0^{2,3}}{4b^2}(e^{-ibt}-1+ibt),\\
f^{(2,3)}_{|220\rangle_{\rm TLR}\otimes|000\rangle_q} &= \frac{\beta_0^{1,2}\beta_0^{1,2}(e^{2iat}-2e^{iat}+1)}{4a^2} + \frac{\beta_0^{1,2}\beta_0^{2,3}\beta_0^{1,3}}{4a^2}\left(\frac{1-e^{2iat}}{2(a+b)} + \frac{e^{iat}-1}{b} + \frac{a^2(1-e^{ict})}{bc(a+b)}\right)\\
&\quad + \frac{\beta_0^{1,2}\beta_0^{2,3}\beta_0^{1,3}}{4ba}\left(\frac{(2a+b)(1-e^{2iat})}{2a(a+b)} + \frac{b(1-e^{ict})}{c(a+c)} + \frac{(a-c)(1-e^{iat})}{ac} + \frac{e^{i(a+c)t}-1}{c}\right),\\
f^{(2,3)}_{|022\rangle_{\rm TLR}\otimes|000\rangle_q} &= \frac{\beta_0^{1,2}\beta_0^{1,2}(e^{2ibt}-2e^{ibt}+1)}{4b^2} + \frac{\beta_0^{1,2}\beta_0^{2,3}\beta_0^{1,3}}{4b^2}\left(\frac{1-e^{2ibt}}{2(a+b)} + \frac{e^{ibt}-1}{a} - \frac{b^2(1-e^{-ict})}{ac(a+b)}\right)\\
&\quad + \frac{\beta_0^{1,2}\beta_0^{2,3}\beta_0^{1,3}}{4ba}\left(\frac{(2b+a)(1-e^{2ibt})}{2b(a+b)} - \frac{a(1-e^{-ict})}{c(b-c)} - \frac{(b+c)(1-e^{ibt})}{bc} - \frac{e^{i(a-c)t}-1}{c}\right),\\
f^{(2,3)}_{|121\rangle_{\rm TLR}\otimes|000\rangle_q} &= \frac{\sqrt{2}\beta_0^{12}\beta_0^{23}}{4ab}(1-e^{iat})(1-e^{ibt}) + \frac{\sqrt{2}\beta_0^{12}\beta_0^{12}\beta_0^{13}}{8a}\left(\frac{1-e^{i(a+b)t}}{ab} + \frac{(e^{ibt}-1)(2c-a)}{abc} + \frac{e^{-ict}-1}{ac}\right.\\
&\quad \left. + \frac{(e^{iat}-1)(b+c)}{abc}\right) + \frac{\sqrt{2}\beta_0^{2,3}\beta 2,3\beta_0^{13}}{8b}\left(\frac{1-e^{i(a+b)t}}{ab} + \frac{(e^{iat}-1)(2c+a)}{abc} - \frac{e^{ict}-1}{ac} - \frac{(e^{iat}-1)(b-c)}{abc}\right),
\end{aligned} \tag{A3}
$$

$$
\begin{aligned}
f^{(3)}_{|000\rangle_{\rm TLR}\otimes|011\rangle_q} &= \frac{\beta_0^{2,3}G_2G_3}{b^3}(1-e^{ibt}+bt(i-0.5bt)),\quad f^{(3)}_{|000\rangle_{\rm TLR}\otimes|110\rangle_q} = \frac{\beta_0^{1,2}G_1G_2}{a^3}(1-e^{iat}+at(i-0.5at)),\\
f^{(3)}_{|330\rangle_{\rm TLR}\otimes|000\rangle_q} &= \frac{\beta_0^{1,2}\beta_0^{1,2}\beta_0^{1,2}}{8a^3}(1-e^{3iat}-3e^{iat}+3e^{2iat}),\quad f^{(3)}_{|033\rangle_{\rm TLR}\otimes|000\rangle_q} = \frac{\beta_0^{2,3}\beta_0^{2,3}\beta_0^{2,3}}{8b^3}(1-e^{3ibt}-3e^{ibt}+3e^{2ibt}),\\
f^{(3)}_{|021\rangle_{\rm TLR}\otimes|001\rangle_q} &= \frac{\sqrt{2}\beta_0^{2,3}\beta_0^{2,3}G_3}{4b^3}(e^{ibt}-1)(1-e^{ibt}+ibt),\quad f^{(3)}_{|210\rangle_{\rm TLR}\otimes|010\rangle_q} = \frac{\sqrt{2}\beta_0^{1,2}\beta_0^{1,2}G_2}{4a^3}(e^{iat}-1)(1-e^{iat}+iat),\\
f^{(3)}_{|120\rangle_{\rm TLR}\otimes|100\rangle_q} &= \frac{\sqrt{2}\beta_0^{1,2}\beta_0^{1,2}G_1}{4a^3}(e^{iat}-1)(1-e^{iat}+iat),\quad f^{(3)}_{|012\rangle_{\rm TLR}\otimes|010\rangle_q} = \frac{\sqrt{2}\beta_0^{2,3}\beta_0^{2,3}G_2}{4b^3}(e^{ibt}-1)(1-e^{ibt}+ibt),\\
f^{(1,2,3)}_{|110\rangle_{\rm TLR}\otimes|000\rangle_q} &= \frac{\beta_0^{12}}{2a}(1-e^{iat}) + \frac{\beta_0^{2,3}\beta_0^{13}}{4b}\left(\frac{e^{iat}-1}{a} + \frac{1-e^{ict}}{c}\right) + \frac{\beta_0^{1,2}\left(G_1^2+G_2^2\right)}{2a^3}\left(1-e^{iat}+iat-\frac{1}{2}a^2t^2\right) - \frac{\beta_0^{1,2}\left(\beta_0^{2,3}\right)^2}{8b}\\
&\quad \times\left(\frac{ite^{iat}}{a}\right) + \frac{\beta_0^{1,2}\left(\beta_0^{2,3}\right)^2}{4a}\left(\frac{1-e^{iat}}{a(a+b)} + \frac{(e^{-ibt}-1)a}{b^2(b+a)} + \frac{it}{b}\right) + \frac{\beta_0^{1,2}\left(\beta_0^{1,3}\right)^2}{8a}\left(\frac{1-e^{iat}}{ab} + \frac{(e^{ict}-1)(b+c)}{c^2b} - \frac{it}{c}\right)\\
&\quad + \frac{\beta_0^{1,2}\left(\beta_0^{2,3}\right)^2}{8b}\left(\frac{(e^{iat}-1)(a+b)}{a^2b} + \frac{1-e^{ict}}{bc}\right) + \frac{\beta_0^{1,2}\left(\beta_0^{2,3}\right)^2}{4ab}\left(\frac{e^{-ibt}-e^{iat}}{a+b} + \frac{e^{ict}-1}{c}\right)\\
&\quad + \frac{\left(\beta_0^{1,2}\right)^3}{4a^3}(2iat+e^{-iat}-e^{iat}) + \frac{\left(\beta_0^{1,2}\right)^3}{8a^3}((2-iat)e^{iat}-(2+iat)),\\
f^{(1,2,3)}_{|011\rangle_{\rm TLR}\otimes|000\rangle_q} &= \frac{\beta_0^{2,3}}{2b}(1-e^{ibt}) + \frac{\beta_0^{1,2}\beta_0^{13}}{4a}\left(\frac{e^{ibt}-1}{b} - \frac{1-e^{-ict}}{c}\right) + \frac{\beta_0^{2,3}\left(G_3^2+G_2^2\right)}{2b^3}\left(1-e^{ibt}+ibt-\frac{1}{2}b^2t^2\right) - \frac{\beta_0^{2,3}\left(\beta_0^{1,2}\right)^2}{8a}\\
&\quad \times\left(\frac{ite^{ibt}}{b}\right) + \frac{\beta_0^{2,3}\left(\beta_0^{1,2}\right)^2}{4b}\left(\frac{1-e^{ibt}}{b(a+b)} + \frac{(e^{-iat}-1)b}{a^2(b+a)} + \frac{it}{a}\right) + \frac{\beta_0^{2,3}\left(\beta_0^{1,3}\right)^2}{8b}\left(\frac{1-e^{ibt}}{ab} + \frac{(e^{-ict}-1)(a-c)}{c^2a} + \frac{it}{c}\right)\\
&\quad + \frac{\beta_0^{2,3}\left(\beta_0^{1,2}\right)^2}{8a}\left(\frac{(e^{ibt}-1)(a+b)}{b^2a} - \frac{1-e^{-ict}}{ac}\right) + \frac{\beta_0^{2,3}\left(\beta_0^{1,3}\right)^2}{4ab}\left(\frac{e^{-iat}-e^{ibt}}{a+b} - \frac{e^{-ict}-1}{c}\right)\\
&\quad + \frac{\left(\beta_0^{2,3}\right)^3}{4b^3}(2ibt+e^{-ibt}-e^{ibt}) + \frac{\left(\beta_0^{2,3}\right)^3}{8b^3}((2-ibt)e^{ibt}-(2+ibt)),
\end{aligned} \tag{A4}
$$

where $a = \Omega_1 + \Omega_2$, $b = \Omega_2 + \Omega_3$, and $c = \Omega_1 - \Omega_3$.

[1] V. V. Dodonov, Phys. Scr. **82**, 038105 (2010).
[2] D. A. R. Dalvit, P. A. M. Neto, and F. D. Mazzitelli, *Lecture Notes in Physics* (Springer, Berlin, 2011), Vol. 834 , p. 419.
[3] G. T. Moore, J. Math. Phys. **11**, 2679 (1970).
[4] S. A. Fulling and P. C. W. Davies, Proc. R. Soc. London, Ser. A **348**, 393 (1976).
[5] E. Yablonovitch, Phys. Rev. Lett. **62**, 1742 (1989).
[6] M. Uhlmann, G. Plunien, R. Schützhold, and G. Soff, Phys. Rev. Lett. **93**, 193601 (2004).
[7] C. M. Wilson, G. Johansson, A. Pourkabirian, M. Simoen, J. R. Johansson, T. Duty, F. Nori, and P. Delsing, Nature (London) **479**, 376 (2011).
[8] J. R. Johansson, G. Johansson, C. M. Wilson, P. Delsing, and F. Nori, Phys. Rev. A **87**, 043804 (2013).
[9] M. A. Andreata and V. V. Dodonov, J. Opt. B **7**, S11 (2005).
[10] A. V. Dodonov and V. V. Dodonov, Phys. Rev. A **85**, 055805 (2012).
[11] S. Felicetti, M. Sanz, L. Lamata, G. Romero, G. Johansson, P. Delsing, and E. Solano, Phys. Rev. Lett. **113**, 093602 (2014).
[12] C. Sabín, I. Fuentes, and G. Johansson, Phys. Rev. A **92**, 012314 (2015).
[13] D. N. Samos-Saénz de Buruaga and C. Sabín, Phys. Rev. A **95**, 022307 (2017).
[14] H. Ollivier and W. H. Zurek, Phys. Rev. Lett. **88**, 017901 (2001).
[15] H. M. Wiseman, S. J. Jones, and A. C. Doherty, Phys. Rev. Lett. **98**, 140402 (2007).
[16] S. J. Jones, H. M. Wiseman, and A. C. Doherty, Phys. Rev. A **76**, 052116 (2007).
[17] E. G. Cavalcanti, S. J. Jones, H. M. Wiseman, and M. D. Reid, Phys. Rev. A **80**, 032112 (2009).
[18] M. H. Wang, X. W. Deng, Z. Z. Qin, and X. L. Su, Phys. Rev. A **100**, 022328 (2019).
[19] M. Wang, Y. Xiang, H. Kang, D. Han, Y. Liu, Q. He, Q. Gong, X. Su, and K. Peng, Phys. Rev. Lett. **125**, 260506 (2020).
[20] X. W. Deng, C. X. Tian, M. H. Wang, Z. Z. Qin, and X. L. Su, Opt. Commun. **421**, 14 (2018).
[21] X. W. Deng, Y. Liu, M. H. Wang, X. L. Su, and K. C. Peng, npj Quantum Inf. **7**, 65 (2021).
[22] P. D. Nation, J. R. Johansson, M. P. Blencowe, and F. Nori, Rev. Mod. Phys. **84**, 1 (2012).
[23] S. Ashhab, A. O. Niskanen, K. Harrabi, Y. Nakamura, T. Picot, P. C. de Groot, C. J. P. M. Harmans, J. E. Mooij, and F. Nori, Phys. Rev. B **77**, 014510 (2008).
[24] F. Helmer, M. Mariantoni, A. G. Flowler, J. von Delft, E. Solano, and F. Marquardt, Europhys. Lett. **85**, 50007 (2009).
[25] A. Galiautdinov, A. N. Korotkov, and J. M. Martinis, Phys. Rev. A **85**, 042321 (2012).
[26] C. K. Andersen and K. Mølmer, Phys. Rev. A **91**, 023828 (2015).
[27] G. Benenti, A. D'Arrigo, S. Siccardi, and G. Strini, Phys. Rev. A **90**, 052313 (2014).
[28] X. Deng, Y. Xiang, C. Tian, G. Adesso, Q. He, Q. Gong, X. Su, C. Xie, and K. Peng, Phys. Rev. Lett. **118**, 230501 (2017).
[29] Y. Xiang, Y. Liu, Y. Cai, F. Li, Y. Zhang, and Q. He, Phys. Rev. A **101**, 053834 (2020).
[30] J. C. Wang, J. L. Jing, and H. Fan, Ann. Phys. **530**, 1700261 (2018).
[31] E. Schrödinger, Proc. Cambridge Philos. Soc. **31**, 555 (1935).
[32] A. Einstein, B. Podolsky, and N. Rosen, Phys. Rev. **47**, 777 (1935).
[33] M. D. Reid, Phys. Rev. A **40**, 913 (1989).
[34] J. S. Bell, Physics **1**, 195 (1964).
[35] N. Brunner, D. Cavalcanti, S. Pironio, V. Scarani, and S. Wehner, Rev. Mod. Phys. **86**, 419 (2014).
[36] M. D. Reid, P. D. Drummond, W. P. Bowen, E. G. Cavalcanti, P. K. Lam, H. A. Bachor, U. L. Andersen, and G. Leuchs, Rev. Mod. Phys. **81**, 1727 (2009).
[37] D. Cavalcanti and P. Skrzypczyk, Rep. Prog. Phys. **80**, 024001 (2017).
[38] M. Piani and J. Watrous, Phys. Rev. Lett. **114**, 060404 (2015).
[39] M. Tomamichel and R. Renner, Phys. Rev. Lett. **106**, 110506 (2011).
[40] C. Branciard, E. G. Cavalcanti, S. P. Walborn, V. Scarani, and H. M. Wiseman, Phys. Rev. A **85**, 010301(R) (2012).
[41] N. Walk, S. Hosseini, J. Geng, O. Thearle, J. Y. Haw, S. Armstrong, S. M. Assad, J. Janousek, T. C. Ralph, T. Symul, H. M. Wiseman, and P. K. Lam, Optica **3**, 634 (2016).
[42] T. Gehring, V. Händchen, J. Duhme, F. Furrer, T. Franz, C. Pacher, R. F. Werner, and R. Schnabel, Nat. Commun. **6**, 8795 (2015).
[43] R. Gallego and L. Aolita, Phys. Rev. X **5**, 041008 (2015).
[44] M. D. Reid, Phys. Rev. A **88**, 062338 (2013).
[45] Q. He, L. Rosales-Zárate, G. Adesso, and M. D. Reid, Phys. Rev. Lett. **115**, 180502 (2015).
[46] C.-Y. Chiu, N. Lambert, Teh-Lu Liao, F. Nori, and C.-M. Li, npj Quantum Inf. **2**, 16020 (2016).
[47] T. P. Orlando and K. A. Delin, *Foundations of Applied Superconductivity* (Addison-Wesley, Reading, MA, 1991).
[48] D. Z. Rossatto, S. Felicetti, H. Eneriz, E. Rico, M. Sanz, and E. Solano, Phys. Rev. B **93**, 094514 (2016).
[49] H. T. Tan, X. C. Zhang, and G. X. Li, Phys. Rev. A **91**, 032121 (2015).
[50] E. G. Cavalcanti, Q. Y. He, M. D. Reid, and H. M. Wiseman, Phys. Rev. A **84**, 032115 (2011).
[51] N. F. Del Grosso, F. C. Lombardo, and P. I. Villar, Phys. Rev. D **102**, 125008 (2020).
[52] Y. Xiang, I. Kogias, G. Adesso, and Q. He, Phys. Rev. A **95**, 010101(R) (2017).
[53] M. Paternostro, W. Son, and M. S. Kim, Phys. Rev. Lett. **92**, 197901 (2004).
[54] M. Wang, Z. Qin, Y. Wang, and X. Su, Phys. Rev. A **96**, 022307 (2017).